Turkish Journal of Electrical Engineering & Computer Sciences

http://journals.tubitak.gov.tr/elektrik/

Research Article

Turk J Elec Eng & Comp Sci
(2014) 22: 1463 – 1475

doi:10.3906/elk-1207-45

A comparison of fuzzy logic and PID controllers to control transmitted power using a TCSC

Mohsen Hosseinzadeh SORESHJANI, Navid Reza ABJADI*,
Abbas KARGAR, Gholamreza Arab MARKADEH
Faculty of Engineering, Shahrekord University, Shahrekord, Iran

Received: 15.07.2012 • **Accepted:** 04.12.2012 • **Published Online:** 07.11.2014 • **Printed:** 28.11.2014

Abstract: Nowadays, the use of flexible AC transmission systems (FACTS) is an economical and interesting approach to improve power transfer capability. The thyristor-controlled series capacitor, as a member of the FACTS family, can control interrelated parameters with dynamism due to its ability of rapid control and stabilization. Regardless of all of the works in this area, the control of transmitted power through the design of the firing angle controller is still missing. In this paper, first, the open-loop firing angle controller and its sensitivities are analyzed to fill in this gap. Next, closed-loop controllers such as PID and fuzzy controllers are designed and simulated in MATLAB/Simulink software. Simulation results show that the fuzzy logic controller has a better response, although it is designed with minimum, simple, triangle membership functions and reduced rule bases.

Key words: FACTS, thyristor-controlled series capacitor, control power flow, fuzzy logic controller.

1. Introduction

The main purpose of power systems is to feed growing loads with the lowest cost, highest reliability, and maximum efficiency. On the other hand, power flow control is a critical issue in the management and utilization of power systems. In recent years, great demand has been imposed, and it is difficult to construct new transmission lines due to financial and environmental issues. In this respect, flexible AC transmission systems (FACTS) technology has been proposed to provide the actual capacity without the requirement of new transmission lines or reconfiguration [1]. The thyristor-controlled series capacitor (TCSC), as a significant member of the FACTS family, has been applied to solve diverse problems, such as scheduling fast power flow, limiting short-circuit currents, regulating continuous reactance, mitigating subsynchronous resonance (SSR), damping the power oscillation, or enhancing transient stability [1–17].

In [3,4], a complete load flow model for the TCSC was proposed by considering all of the harmonics of line currents. A variety of model-based control schemes can be found in [5–7], which express the adaptability at higher frequencies and are useful in SSR studies. In [8–13], it was demonstrated that the TCSC can be employed to improve transient stability, and several nonlinear controllers were designed. Much attention has been paid to improve transient stability using the TCSC. To the best of our knowledge, no research work has considered the TCSC for controlling transmitted active power. This paper is related to the way of applying the TCSC for controlling transmitted power through the firing angles.

*Correspondence: navidabjadi@yahoo.com

The conventional proportional-integral-derivative (PID) controller is widely employed in industrial applications and control processes because of its simplicity, clear functionality, and feasibility. However, it is not usually able to give a satisfactory performance when applied to nonlinear systems. A power system with a TCSC has a nonlinear characteristic, and using PID control deteriorates the performance of the system.

The application of artificial intelligence methods in power systems is interesting and motivating. Among these methods, a fuzzy logic controller (FLC) can be designed based on human knowledge when system mathematical models are unknown or complicated because of nonlinear characteristics and uncertainties, and a suitable FLC can overcome environmental variations during operation [18]. Thus, in the past 3 decades, FLCs have replaced conventional controllers in many applications and industries.

In [14], the control of the load voltage in the presence of a TCSC by a PID controller and FLC was proposed, and the impact of these controllers on the total harmonic distortion (THD) in the load voltage and current were compared for various loads. The simulation results in [14] showed that a network with a TCSC using an FLC had a better response compared to a PID controller. In [15–17,19], several fuzzy TCSC damping controllers were designed and investigated to improve power system stability.

In this paper, first, the role of a TCSC on power flow control is discussed, and an open-loop controller, which is designed based on power flow relationships, is analyzed, and then a conventional PID controller as the simplest closed-loop controller is designed. Finally, a FLC with minimum rules and triangular membership functions is designed, and its performance is compared to the PID controller for 2 different cases.

2. Transmitted power control using a TCSC

The TCSC is the simplest classical and most economical FACTS device that provides transmitted power rapidly and accurately. In addition, a TCSC offers smooth and flexible control of the transmitted active power.

Thyristor-switched series capacitance and thyristor-switched series reactance operate like the TCSC, but they are not able to control the transmitted power accurately, because they are discrete devices.

A phase-shifting transformer (PST) is the main device for power flow control. Nevertheless, the PST cannot rapidly react, and its operation is limited only for steady states. It is worthwhile to note that the TCSC is more economical than the PST because of its transformer. Moreover, the PST cannot continuously provide transmitted power.

Other approaches such as the static synchronous series compensator, hybrid flow controller (HFC), rotary power flow controller, and unified power flow controller have definitive merits, but their usages are not widespread because of cost considerations.

In this paper, the studied system is a power system compensated by a TCSC. In this study, since the total demand and generation are fixed, the dynamic of the generators is neglected, so the voltage on each side and the transmission angle δ are fixed. A single-line diagram of the test system is shown in Figure 1, where the transmission line is represented by a lumped inductive reactance, X_{10-11}, in accordance with the approach for the power flow model of the HFC [20]. With respect to buses i and j (Figure 1), the power network is represented by the corresponding Thevenin equivalents, V_S, jX_1 and V_r, jX_2, respectively [21].

Ignoring the line charging and losses, P, the active power flow, is given by:

$$P = \frac{V_S V_r}{X_{Sys} + X_{TCSC}} Sin\delta, \tag{1}$$

where X_{Sys} is the equivalent system's reactance when the TCSC is bypassed. The power flow throughout

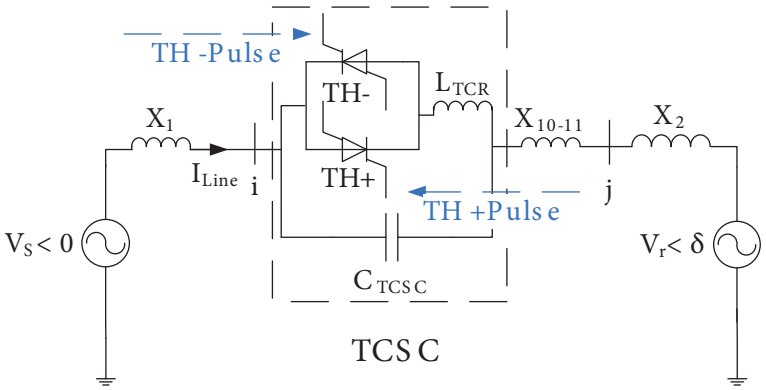

Figure 1. Single-line diagram of the test system compensated by a TCSC.

the network is mainly distributed as a function of the series impedance. X_{TCSC} is controlled by the firing angle of the thyristors. Consequently, the transmitted active power can be controlled by the firing angle. The relationship between X_{TCSC} and the firing angle is given by:

$$X_{TCSC} = \frac{X_C X_{TCR}(\alpha)}{X_{TCR}(\alpha) + X_C}, \tag{2}$$

$$X_{TCR}(\alpha) = 2\pi f L \frac{\pi}{\pi - 2\alpha - \sin 2\alpha}, \tag{3}$$

where X_{TCR} is the inductive reactance corresponding to the fundamental harmonic and α is the firing angle that is synchronized with the line current, so it varies in the range of 0° to 90° [2].

There are also some attempts to derive an accurate model of the TCSC considering harmonics [1–6]. In [1], X_{TCSC} was obtained as follows:

$$X_{TCSC} = -X_C + C_1 \left(2\beta + \sin_{2\beta}\right) - C_2 \cos^2_{\beta} \left(\lambda \tan_{\lambda\beta} - \tan \beta\right), \tag{4}$$

where

$$C_1 = \frac{X_C + X_{LC}}{\pi}, \tag{5}$$

$$C_2 = \frac{4X_{LC}^2}{\pi X_L}, \tag{6}$$

$$\lambda = \sqrt{\frac{X_C}{X_L}}, \tag{7}$$

$$\beta = \frac{\pi}{2} - \alpha, \tag{8}$$

$$X_{LC} = \frac{X_C X_L}{X_C - X_L}. \tag{9}$$

The parameters of the TCSC are selected so that the control of the transmitted active power can continuously be possible in the order of megawatts, and it is required that the TCSC operates in both capacitive and inductive modes. C_{TCSC} can be determined based on the necessary reactance in $\alpha = 90^\circ$. The desired performance of the TCSC in both inductive and capacitive modes will be achieved by selecting $\lambda = 2.5$ and L_{TCR} can be determined straightforward. The TCSC's parameters, which are used in the simulation, are listed in Table 1.

The variation of X_{TCSC} as a function of α, for the parameters of Table 1, is shown in Figure 2, which compares X_{TCSC} obtained from Eqs. (2) and (4).

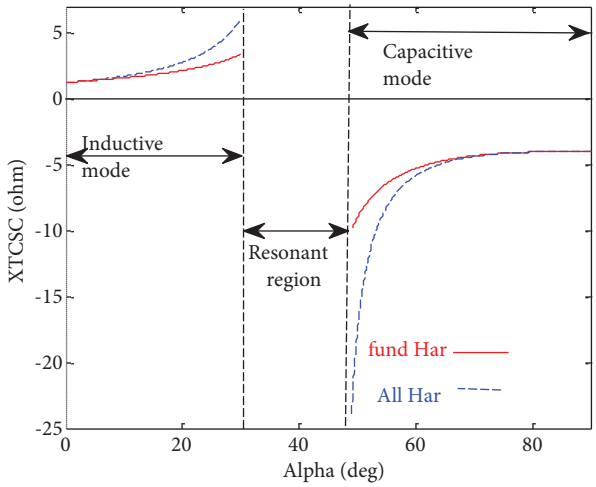

Figure 2. Relationship between X_{TCSC} and α.

Table 1. TCSC's parameters.

Parameter	Value
L_{TCR}(mH)	2.5
C_{TCSC} (μF)	663
$C_{Snub.}$ (nF)	50
$R_{Snub.}$ (kΩ)	5

Operation with α close to the resonance region is not safe since X_{TCSC} is infinite theoretically and more harmonics may be generated; therefore, a limiter is desirable to avoid entering the resonant region. One may note that, by decreasing α from the resonant region, the TCSC operates in inductive mode, as well as in capacitive mode when α is larger than the resonant region. In this paper, the TCSC is employed only with capacitive mode solely to increase the transmitted power, and inductive mode is used to prevent overflow. Hence, a limiter should restrict α between 49 and 90; thus, the first α is 90. After that, the firing angle controller is activated by decreasing α to increase the transmitted active power gradually. If a higher rating of TCSC is used, it would be more expensive, and the harmonic injection would be higher.

3. Open-loop controller

According to Eq. (1), the firing angle is directly obtained from the load flow analysis and an open-loop controller can be designed to control the active power flow. The sensitivity of this controller can be expressed as follows.

The sensitivity of P with respect to the system reactance, X_{Sys}, based on Eq. (1), is given by:

$$\frac{\partial P}{\partial X_{Sys}} = \frac{-P}{X_{Sys} + X_{TCSC}}. \tag{10}$$

Thus, P is very sensitive to X_{Sys} and X_{TCSC}. As X_{TCSC} is related to α, P is very sensitive to α. In [4],

determining the arrays of the Jacobean matrix, $\frac{\partial P}{\partial \alpha}$, the sensitivity to the operation point is given by:

$$\frac{\partial P}{\partial \alpha} = \frac{-P}{X_{Sys} + X_{TCSC}} \frac{\partial X_{TCSC}}{\partial \alpha}. \tag{11}$$

Moreover, it can be shown that by changing the firing angle, the reactive power changes as well:

$$\frac{\partial Q}{\partial \alpha} = \frac{-Q}{X_{Sys} + X_{TCSC}} \frac{\partial X_{TCSC}}{\partial \alpha}. \tag{12}$$

From Eqs. (11) and (12), one can conclude that with the TCSC, it is not possible to control the active power independent of the reactive power. Considering the fundamental harmonic, one can obtain:

$$\frac{\partial X_{TCSC}}{\partial \alpha} = \frac{\partial X_{TCSC}}{\partial X_{TCR}} \frac{\partial X_{TCR}}{\partial \alpha}, \tag{13}$$

$$\frac{\partial X_{TCSC}}{\partial \alpha} = \frac{-X_C^2}{(X_{TCR} - X_C)^2} \frac{4\pi^2 f L_{TCR}(1 + \cos_{2\alpha})}{-2\pi \sin_{2\alpha} + 4\alpha \sin_{2\alpha} + \pi^2 - 4\pi\alpha + 4\alpha^2 - \cos^2_{2\alpha} + 1}. \tag{14}$$

Considering the harmonics, Eq. (14) is changed to:

$$\frac{\partial X_{TCSC}}{\partial \alpha} = -2C_1 (1 - \cos_{2\alpha}) - C_2 \sin_{2\alpha} \left\{ \lambda \tan_{\lambda(\frac{\pi}{2} - \alpha)} - \tan_{\frac{\pi}{2} + \alpha} \right\} + C_2 \left\{ \lambda^2 \frac{\cos^2_{\frac{\pi}{2} - \alpha}}{\cos^2_{\lambda(\frac{\pi}{2} - \alpha)}} - 1 \right\}. \tag{15}$$

To have a better look at the differences of Eqs. (14) and (15), $\frac{\partial X_{TCSC}}{\partial \alpha}$ is depicted in Figure 3, using the parameters given in Table 1 for both cases.

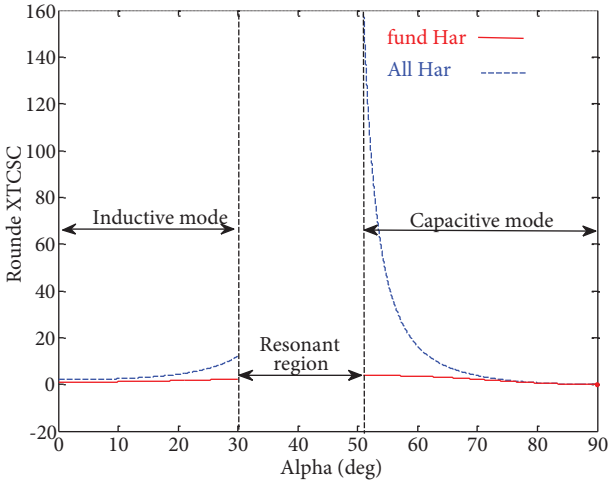

Figure 3. $\frac{\partial X_{TCSC}}{\partial \alpha}$ for the first harmonic and all of the harmonics.

Thus, only closed-loop controllers should be designed because:

- The open-loop controller is sensitive to the change of parameters and operating point, and the system parameter uncertainty leads to poor performance of the controller.

- Eq. (1) is related to the steady state and is not suitable for the transient state.
- The error of the open-loop controller in the presence of harmonics will be high, due to the need to measure the angle and amplitude of the voltage first harmonic on each side.
- Owing to the lack of an accurate model of the TCSC and the various models for different conditions, finding an accurate inverse relationship would not be possible to feasibly determine α.

The use of closed-loop control makes the response relatively insensitive to external disturbances and internal variations in the system parameters, and it increases the bandwidth for control purposes.

4. PID controller

Here, a conventional PID controller as the simplest closed-loop controller is designed to determine the firing angle to control the transmitted power. For this purpose, first, the power error signal, which is the difference of the reference and measured powers, is determined by Eq. (16):

$$e = P_{Ref} - P_{Meas}. \tag{16}$$

The firing angle is the output of the PID controller when it is limited in capacitive mode, as shown in Figure 4. Moreover, the firing pulses of each phase should be synchronized by the line current of the same phase.

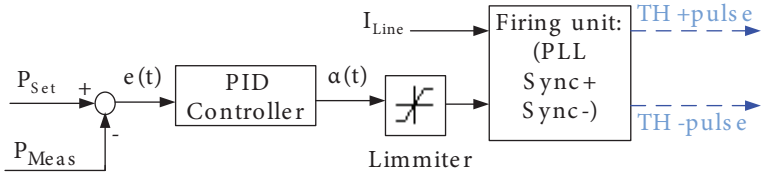

Figure 4. Structure of the PID controller to determine the firing pulses of the TCSC.

The PID output is given by:

$$\alpha(t) = k_P e(t) + k_i \int_0^t e(t)dt + k_d \frac{de(t)}{dt}, \tag{17}$$

where k_p, k_i, and k_d are the proportional, integral, and derivative constant gains, respectively. In this paper, we tune these parameters by the Ziegler–Nichols method. In this method, k_i and k_d are considered as 0; then k_p is increased from 0 to a critical value, Kcr, where the system has just become unstable or the output has oscillatory behavior. Kcr and the period of oscillations, Pu, are useful to determine the coefficients of a PID controller as follows:

$$\begin{cases} k_p = \frac{3}{5}Kcr \\ k_i = \frac{6Kcr}{5Pu} \\ k_d = \frac{3KcrPu}{40} \end{cases}. \tag{18}$$

The Ziegler–Nichols method suggests some rules to set the gains of a PID controller according to Eq. (18). However, the final coefficients of a PID controller are not equal to these rules, but it is a good initial point for tuning the parameters. Tuning the PID controller, especially in the presence of disturbances, is difficult and cumbersome. As mentioned earlier, the performance of PID controllers may not be suitable due to the nonlinear

characteristic of the TCSC. With the passing of time, the system's parameters may change and lead to a change of the operating point, and tuning the controller gains is necessary. Furthermore, in industrial applications, to eliminate high-frequency noise, a low-pass filter is combined with the derivative term and the construction of an ideal PID controller in practice is almost impossible. Moreover, the operation of the conventional PID controller is not satisfied for different references.

5. Fuzzy PI+D controller

Due to imperfections of PID controllers, the possibility of replacing a PID controller with the FLC is proposed [18]. Since human knowledge is used for designing fuzzy controllers, there are many ways to design FLCs. Nevertheless, here, to design a firing angle controller, a simple fuzzy PI+D controller is used, and it is implemented by the Fuzzy Inference System toolbox in MATLAB/Simulink software. The firing angle is obtained by limiting the output of the fuzzy PI+D controller in capacitive mode, while the input limiters put the variables in the normalized range. The schematic of the fuzzy PI+D is shown in Figure 5 in detail, and $\alpha\,[n]$,the output of the fuzzy PI+D at time n, is given by:

$$\alpha\,[n] = \alpha\,[n-1] + \Delta\alpha\,[n] + G_4\Delta e\,[n]\,. \tag{19}$$

In Eq. (19),$\Delta\alpha[n]$ is the output of the fuzzy system, $\alpha\,[n-1]$ is the firing angle of the previous instant, and $G4$ is the gain of the derivative term. The term of $\Delta e[n]$ is the error change that can be calculated by Eq. (20), and it plays the role of a derivative term. As a result, the mentioned problems of a derivative are eliminated.

$$\Delta e\,[n] = e1[n] - e1[n-1] \tag{20}$$

Here, $e1[n-1]$ is the previously measured error.

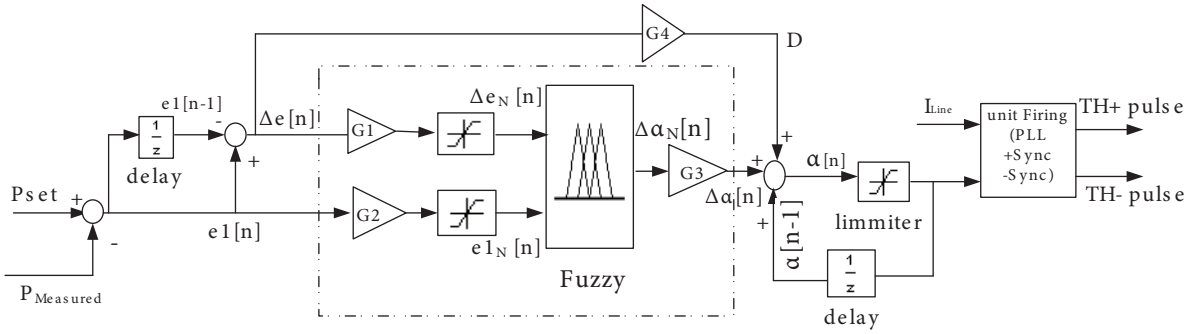

Figure 5. Structure of the fuzzy PI+D controller.

5.1. Fuzzification and defuzzification

The incremental FLC of Figure 5 is a standard one that has 2 inputs, *e1[n]* and $\Delta e1[n]$, and 1 output $\Delta\alpha[n]$. Three scale factors, $G1$, $G2$, and $G3$, are defined to normalize the inputs and denormalize the output. In the normalization process, we scale the input and output values between (–1, +1). However, in the denormalization process, as a result of the nonlinear characteristic of X_{TCSC} (Figure 2), $G3$ should be designed as a gain scheduling (GS) based on a function of $\alpha[n-1]$. In other words, we design the fuzzy PI based on the fuzzy GS and the direct action type. Consequently, we define 3 identical triangle functions for the inputs and the output membership functions named P (positive), Z (zero), and N (negative). These membership functions

are illustrated in Figure 6. The triangle membership function is used as the simplest membership function to show the capability of the fuzzy controller.

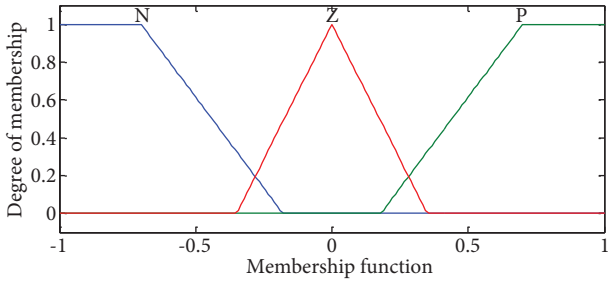

Figure 6. Degrees of the input and output membership functions.

5.2. Fuzzy rules

In this design, we use this fuzzy statement: the firing angle should be changed proportionally to the error or rate of the error when they are nonzero. The general form of the rule bases is expressed as: If *(e is A) and (Δe is B), then the output is C*. The set of rules used in the fuzzy controller is shown in Table 2, and they are derived from general human knowledge. In general, a $3 \times 3 = 9$ rule base can be designed for the FLC. Nevertheless, the number of rules in the controller is reduced from 9 to 5 to reduce the complexity of the controller. The first law is used for the steady state, and a zero-output fuzzy PI is used to retain the previous firing angle; consequently, the final appropriate firing angle is obtained. A fuzzy integrator term is formed using the 2nd and 3rd laws of Table 2. The 4th and 5th laws are used as a proportional term. Figure 7 illustrates the corresponding 3-dimensional control surface in the normalized universe of discourse.

Table 2. Rule set for the fuzzy PI controller.

	e	Δe	$\Delta\alpha$
1	Z	Z	Z
2	P	Z	P
3	N	Z	N
4	Z	P	P
5	Z	N	N

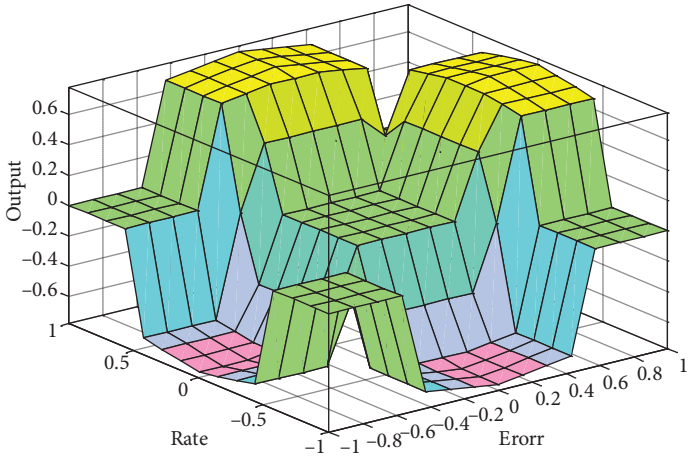

Figure 7. Three-dimensional control surface of the fuzzy PI controller.

5.3. Inference mechanism

The result of the inference mechanism consists of the weighting factor w_i and the alpha changing c_i of the individual rules, which is taken from the rule base. The weighting factor w_i is obtained by Mamdani's min fuzzy implication of $\mu e(e1[n])$ and $\mu\Delta e(\Delta e1\ [n])$, i.e. wi = min$\{\mu e(e1[n]),\ \mu\Delta e(\Delta e1[n])\}$, where $\mu e(e1[n])$, $\mu\Delta e(\Delta e1[n])$ are the degrees of the membership functions. The change in the firing angle of the ith rule, z_i, is given by:

$$z_i = w_i \times c_i = \min\{\mu_e(e\,[n]), \mu_{\Delta e}(\Delta e\,[n])\} \times c_i. \tag{21}$$

In this study, the authors prefer the Mamdani method over the Sugeno method, because it is easier to be computed, more intuitive, and well suited to human input.

5.4. Defuzzification

The center of average method is used to calculate the output of fuzzy system, which is given by:

$$\Delta\alpha_N\,[n] = \frac{\sum_{i=1}^{N} w_i \times c_i}{\sum_{i=1}^{N} w_i}. \tag{22}$$

In Eq. (22), N is the number of active rules. Often, tuning is done for the fuzzy controller by the trial and error method.

6. Simulation results

The PID and FLC performances are compared with a computer simulation. In order to verify these controllers, 2 cases are considered: fundamental and unbalanced voltages in the presence of harmonics. In the transient state, the TCSC is bypassed. In the transient time that takes 0.5 s, the power flow is almost 70 MW. From 0.5 to the first second, the TCSC is considered in the system with $\alpha = 90°$ and the power flow is increased to 76 MW. In t = 1(s), the firing angle controller is activated. Figures 8 and 9 show the power flow in the transmission line and the thyristor's firing angles, respectively, with the PID controller. The conventional PID controller is tuned based on the P_{Set} = 83 (MW) operating condition. Its performance is not satisfactory for different operating points or in the presence of changes in the parameters. When P_{set} is equal to 78 (MW), the transmitted power has an overshoot with considerable variations in the steady state.

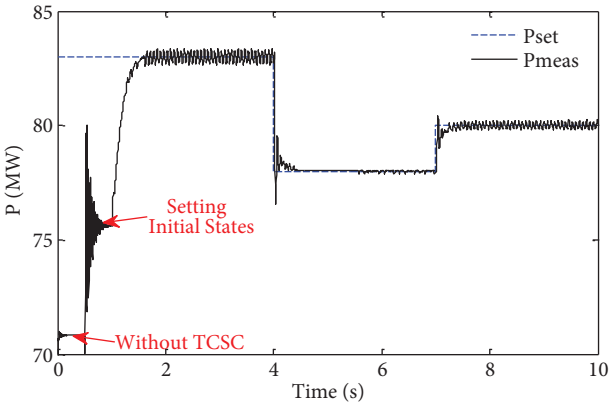

Figure 8. Power variation in the time domain based on the PID controller.

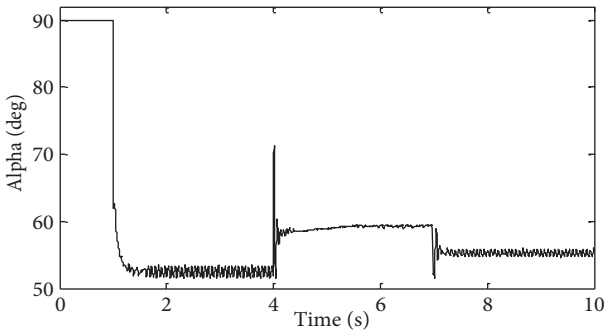

Figure 9. Firing angle variation in the time domain based on the PID controller.

It can be seen from Figures 10 and 11 that the transmitted power ripples are effectively reduced when the FLC is applied. The fuzzy PI+D controller is a soft computing controller, and it has lower action than the PID controller.

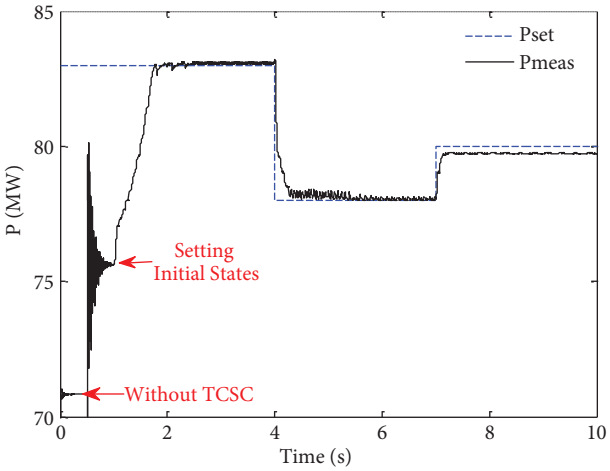

Figure 10. Power variation in the time domain based on the fuzzy PI+D controller.

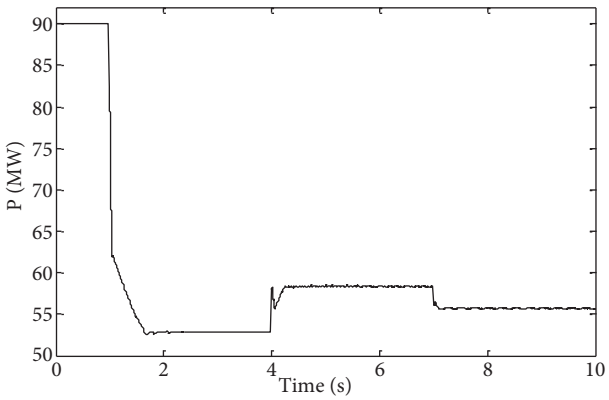

Figure 11. Firing angle variation in the time domain based on the fuzzy PI+D controller.

The transient and steady-state response parameters, such as overshoot, settling time, rise time, steady-state peak-to-peak, and steady-state error values of the transmitted active power, obtained from Figures 9–11, are listed in Tables 3 and 4.

Table 3. Response information based on the PID controller.

Pset	Overshoot (MW)	Rise time (s)	Settling time (s)	S-S error (MW)	S-S peak-to-peak (MW)
83 MW (stage 1)	0	0.5	0.7	0	0.7
78 MW (stage 2)	1.43	0.024	0.45	0	0.2
80 MW (stage 3)	0.413	0.0267	0.5	0	0.4

Table 4. Response information based on the fuzzy PI+D controller.

Pset	Overshoot (MW)	Rise time (s)	Settling time (s)	S-S error (MW)	S-S peak-to-peak (MW)
83 MW (stage 1)	0	0.75	1	0.05	0.06
78 MW (stage 2)	0	0.25	0.5	0	0.12
80 MW (stage 3)	0	0.1	0.2	0.2	0.045

The FLC yields a superior response with respect to the PID controller for most references, with a slight overshoot and an acceptable steady-state error. Robustness with respect to the reference variation is one of the most frequent advantages of the fuzzy controller over the PID controller, which is illustrated by the simulation results. On the other hand, robustness of the designed FLC with respect to the changing parameters is illustrated by a closed-loop system simulation in the presence of harmonics and changing values of X_{Sys}. In other words, the Thevenin voltage on each side of the test system is polluted with an unbalanced voltage with a THD of 15% (contained in the 5th and 7th harmonics) and unbalanced voltages. A series reactance is switched in and out several times at 3, 6, and 8 s, respectively (with step variation of this reactance, we mean that one part of the

power system transmission line is added to the system or bypassed). The simulation results of this test with the PID controller are shown in Figures 12 and 13.

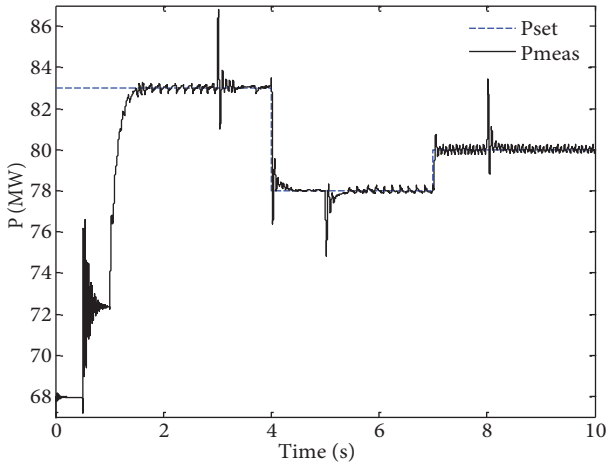

Figure 12. Power variation in the time domain based on the PID controller (considering harmonics and variations of the reactance).

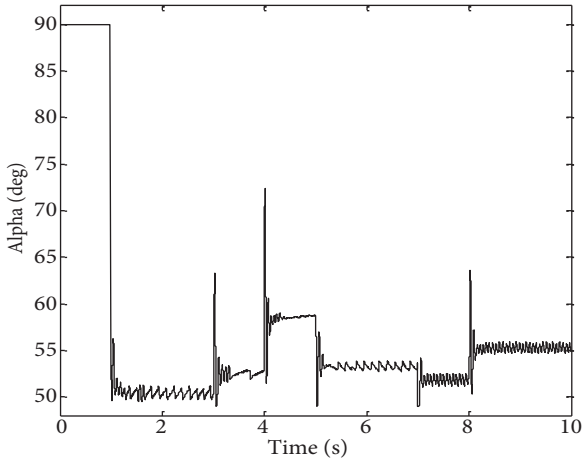

Figure 13. Firing angle variation in the time domain based on the PID controller (considering harmonics and variations of the reactance).

The PID controller can track the transmitted power even in the presence of disturbances, but the fuzzy PI+D operates better than a PID controller because it has no overshoot (see Figures 14 and 15). It is worth noting that the spikes in Figures 14 and 15 are due to the step change of X_{Sys}.

The response performance data from Figures 12–15 are listed in Tables 5 and 6 for both designed controllers.

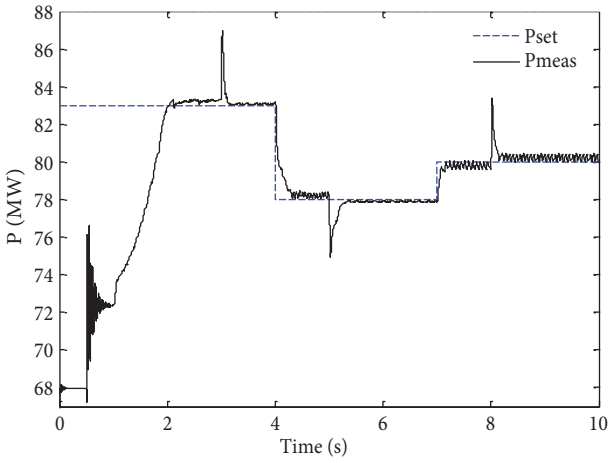

Figure 14. Power variation in the time domain based on the fuzzy PI+D controller for the TCSC (considering harmonics and variations of the reactance).

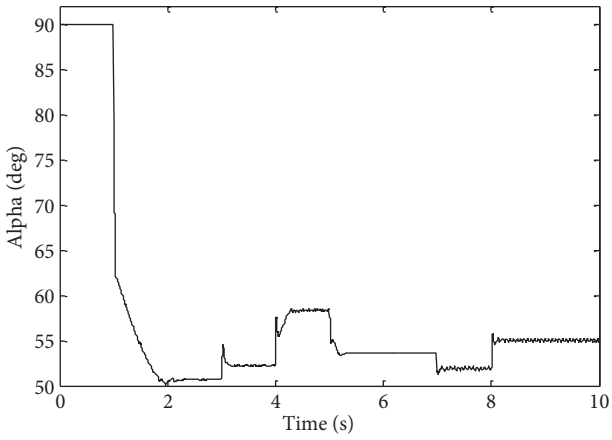

Figure 15. Firing angle variation in the time domain based on the fuzzy PI+D controller (considering harmonics and variations of the reactance).

Table 5. Response information based on the PID controller without harmonics.

Pset	Overshoot (MW)	Rise time (s)	Settling time (s)	S-S error (MW)	S-S peak-to-peak (MW)
83 MW (stage 1)	0	0.5	0.8	0	0.45
83 MW (bypass X_L)	1	0.038	0.45	0	0.38
78 MW (stage 2)	1.43	0.024	0.45	0	0.2
78 MW (switch in)	0.34	0.055	0.5	0	0.35
80 MW (stage 3)	0.75	0.039	0.13	0	0.5
80 MW (bypass X_L)	1.2	0.04	0.3	0	0.4

Table 6. Response information based on the fuzzy PI+D controller (considering harmonics and variations of the reactance).

Pset	Overshoot (MW)	Rise time (s)	Settling time (s)	S-S error (MW)	S-S peak-to-peak (MW)
83 MW (stage 1)	0	1	1	0.05	0.2
83 MW (bypass X_L)	0	0.18	0.18	0.05	.07
78 MW (stage 2)	0	0.3	.3	0.1	0.25
78 MW (switch in)	0	0.4	0.4	0.08	.05
80 MW (stage 3)	0	0.08	0.11	0	0.4
80 MW (bypass X_L)	0	0.17	0.18	0	0.4

7. Conclusion

In this paper, an analysis is given on open-loop control of the transmitted active power using a TCSC in a power transmission line, and its sensitivity to parameter variations is investigated. The performance of the closed-loop TCSC with PID and very simple fuzzy controllers is compared in 2 different cases. The simulation results show that when using a FLC for the TCSC, the transmitted power has less variation and better dynamic response than a PID controller.

References

[1] K.R. Padiyar, FACTS Controllers in Power Transmission and Distribution, Tunbridge Wells, UK, Anshan, 2009.

[2] N.G. Hingurani, L. Gyugyi, Understanding FACTS: Concepts and Technology of Flexible AC Transmission Systems, IEEE Press, New York, Wiley, 2000.

[3] C.R. Fuerte-Esquivel, E. Acha, H. Ambriz-Perez, "A thyristor controlled series compensator model for the power flow solution of practical power networks", IEEE Transactions on Power Systems, Vol. 15, pp. 58–64, 2000.

[4] S. Sreejith, P. Sishaj Simon, M.P. Selvan, "Power flow analysis incorporating firing angle model based TCSC", IEEE Conference on Industrial and Information Systems, pp. 496–501, 2010.

[5] S.R. Joshi, A.M. Kulkarni, "Analysis of SSR performance of TCSC control schemes using a modular high bandwidth discrete-time dynamic model", IEEE Transactions on Power Systems, Vol. 24, pp. 840–848, 2009.

[6] K. Kabiri, S. Henschel, J.R. Marti, H.W. Dommel, "A discrete state space model for SSR stabilizing controller design for TCSC compensated system", IEEE Transactions on Power Delivery, Vol. 20, pp. 466–474, 2005.

[7] S.R. Joshi, E.P. Cheriyan, A.M. Kulkarni, "Output feedback SSR damping controller design based on modular discrete-time dynamic model of TCSC", IET Generation, Transmission & Distribution, Vol. 3, pp. 561–573, 2009.

[8] L. Kejun, J. Zhao, C. Zhang, W.J. Lee, "A study on mode-switching control of TCSC based on conditional firing of Thyristor", IEEE Transactions on Power Delivery, Vol. 26, pp. 1196–1202, 2011.

[9] A.M. Simoes, D.C. Savelli, P.C. Pellanda, N. Martins, P. Apkarian, "Robust design of a TCSC oscillation damping controller in a weak 500-kV interconnection considering multiple power flow scenarios and external disturbances", IEEE Transactions on Power Systems, Vol. 24, pp. 226–236, 2009.

[10] D. Rai, G. Ramakrishna, S.O. Faried, A.A. Edris, "Enhancement of power system dynamics using a phase imbalanced series compensation scheme", IEEE Transactions on Power Systems, Vol. 25, pp. 966–974, 2010.

[11] S. Ray, G.K. Venayagamoorthy, B. Chaudhuri, R. Majumder, "Comparison of adaptive critic-based and classical wide-area controllers for power systems", IEEE Transactions on Power Systems, Vol. 38, pp. 1002–1007, 2008.

[12] D. Rai, S. Faried, G. Ramakrishna, A. Edris, "Damping inter-area oscillations using phase imbalanced series compensation schemes", IEEE Transactions on Power Systems, Vol. 26, pp. 1753–1761, 2011.

[13] J.M. Gonzalez, C.A. Canizares, J.M. Ramirez, "Stability modeling and comparative study of series vectorial compensators", IEEE Transactions on Power Delivery, Vol. 25, pp. 1093–1103, 2010.

[14] U. Yolac, T. Yalcinoz, "Comparison of fuzzy logic and PID controllers for TCSC using MATLAB", 39th International Universities Power Engineering Conference, Vol. 1, pp. 438–442, 2004.

[15] M. Tripathy, S. Mishra, "Interval type-2-based thyristor controlled series capacitor to improve power system stability", IET Generation, Transmission & Distribution, Vol. 5, pp. 209–222, 2011.

[16] P.K. Dash, S.R. Samantaray, G. Panda, "Fault classification and section identification of an advanced series-compensated transmission line using support vector machine", IEEE Transactions on Power Delivery, Vol. 22, pp. 67–73, 2007.

[17] X. Tan, N. Zhang, L. Tong, Z. Wang, "Fuzzy control of thyristor controlled series compensator in power system transients", Fuzzy Sets and Systems, Vol. 110, pp. 429–436, 2000.

[18] D.G. Schwartz, G.J. Klir, H.W. Lewis, Y. Ezawa, "Application of fuzzy sets and approximate reasoning", Proceedings of the IEEE, Vol. 82, pp. 482–498, 1994.

[19] S. Hameed, "Power system stability enhancement using reduced rule base self-tuning fuzzy PI controller for TCSC", IEEE PES Transmission and Distribution Conference and Exposition, pp. 1–8, 2010.

[20] S.A. Nabavi Niaki, R. Iravani, M. Noroozian, "Power-flow model and steady-state analysis of the hybrid flow controller", IEEE Transactions on Power Delivery, Vol. 23, pp. 2330–2338, 2008.

[21] A.A. Afzalian, S.A. Nabavi Niaki, M.R. Iravani, W.M. Wonham, "Discrete-event systems supervisory control for a dynamic flow controller", IEEE Transactions on Power Delivery, Vol. 24, pp. 219–230, 2009.